CHAPTER II

RATIONALE, THEORY AND HYPOTHESIS

The basic concepts of quantum dot (QD) structure, which is a low-dimensional semiconductor nanostructure, are reviewed in this chapter. A comparison of important intrinsic properties of nanostructures is presented. The properties of quantum rings (QRs), a type of quantum-confinement structures, are also reviewed to be useful for the interpretation of nanostructure characteristics.

In another part of this chapter, self-assembled growth of the nanostructures is presented based on epitaxial growth. Self-assembled growth modes are briefly introduced to provide the basics of nanostructure formation from strain-releasing in a lattice mismatch system. The next section, a review of droplet epitaxy which is the lattice-matched method used to fabricate the QRs in this research work is presented. Migration-enhanced epitaxy (MEE) is also briefly introduced. Finally, the information of the material system which is used to create the nanostructures is provided.

2.1 Quantum Nanostructures

The electronic properties for quantum dot (QD) structures differ from the bulk system. While the bulk has a continuous energy band, the low-dimensional nanostructures have discrete energy levels and delta-like density of states due to the carrier confinement and quantization of carrier energy. Hence QD is also called an *artificial atom* for its quantized energy levels like a real atom.

2.1.1 Carrier confinement and energy level quantization

The band theory of crystals has been rigorously developed from the quantum theory for atoms since the last century [30,31]. Figure 2.1 shows a schematic comparison between a bulk semiconductor, a waveguide for visible light, a QD, and an atom. From the quantum theory, we know that an atom has discrete energy levels. Atoms together would become a solid with energy bands. The most relevant bands are the conduction band and the valence band which are separated in energy by the band

gap. At T = 0 K, the conduction band is free of electrons while the valence band is full with electron. At $T > 0$ K, these two bands are partially filled with electrons and holes (carriers in device operations). Controlling the *carrier motion* in these two bands is the subject of band gap engineering.

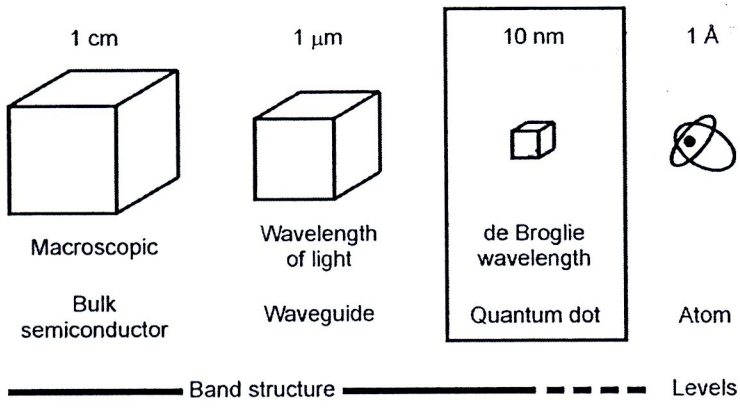

Figure 2.1 Schematic comparison of bulk, waveguide, QD, and atom [32].

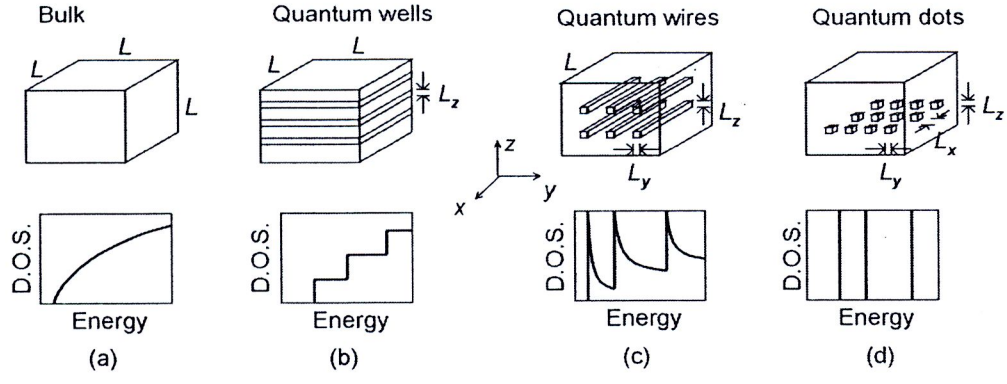

Figure 2.2 Schematic views and graphs of (a) bulk (3-D structure), (b) quantum wells (2-D structure), (c) quantum wires (1-D structure), and (d) QD (0-D structure) and their density of states (D.O.S.) [33]. L is in macroscopic scale (~cm), while L_x, L_y, L_z, are in nanoscale.

Because the structural size is varied continuously, there exists a description between the two cases (discrete levels and continuous band structure). The densities of states of energy band structure of bulk semiconductor and low-dimensional nanostructures are illustrated in figure 2.2 [33]. In the case of QD, since the low-

dimensional-shaped nanostructures provide the potential well resulted from difference of energy band gap (E_g) of 2 materials in the three directions, the carrier motions are completely confined in this 3-D confinement structure and result in a delta function density of states. The specific energy photons would be emitted when the nanostructures are stimulated.

The quantization phenomenon can be described by wave-like properties of confined electrons, since any substance would exhibit its related wave properties. In the low-dimensional nanostructures, most of carriers are confined in one or more directions and the length scale of confining direction is in the order of the de Broglie wavelength (carrier wavelength). The de Broglie wavelength, $\lambda_{\text{de Broglie}}$, depends on the carrier effective mass, m^*, and temperature, T [34]:

$$\lambda_{\text{de Broglie}} = \frac{h}{p} = \frac{h}{\sqrt{3m^* k_B T}} \tag{2.1}$$

where h is Planck's constant, p is carrier momentum, and k_B is Boltzmann's constant.

In a potential well, the confined carriers are limited in their motion, so they look-like stationary. The wave-like properties of a *stationary* electron can be only de Broglie wavelengths which create standing wave within the width of the potential well, that is, the width of the nanostructures. The discrete-values of carrier's de Broglie wavelengths would be exhibited, and cause discrete energy levels in such 3-D confinement structures. A schematic representation of the lowest three levels of carrier energy quantization in a potential well is shown in figure 2.3.

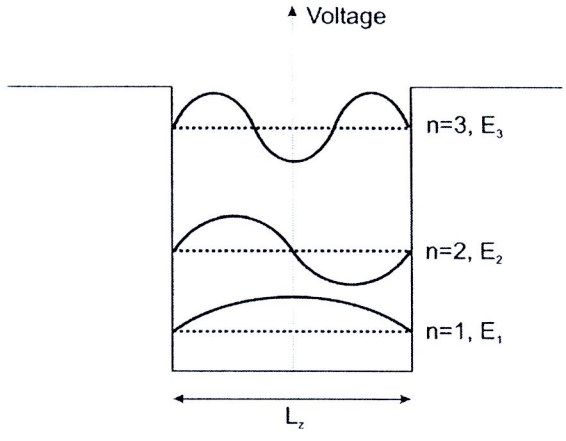

Figure 2.3 The lowest three levels of carrier's energy quantization in a potential well with a width of L_z (comparable to de Broglie wavelength). The picture shows examples of the three lowest-energy standing waves (solid line) which can happen in a potential well and the corresponding carrier's energy level of the de Broglie wavelength from the standing wave (dotted line), i.e. E_1, E_2 and E_3. The energy of each level is given by $E_{n,z} = \hbar^2(n\pi)^2 / 2m^* L_z^2$, where n is an integer number.

In semiconductor quantum structures, the effective-mass approximation is widely used for the quantized energy level calculation as a function of the well width [35]. The main assumption of the effective-mass approximation is that the envelope wave function does not significantly vary in the unit cell with a length scale of subnanometers, therefore this assumption is valid in all low-dimensional nanostructures. Assuming parabolic band dispersion, the band-edge electron states of semiconductors can be described by a Schrödinger-like equation as

$$\left[-\frac{\hbar^2}{2m^*}\nabla^2 + V(\mathbf{r})\right]F(\mathbf{r}) = E\,F(\mathbf{r}) \qquad (2.2)$$

Here, m^* is the effective mass; $\hbar$ is the reduced Planck's constant; $\mathbf{r} = (x,y,z)$ is the carrier position vector; $V(\mathbf{r})$ is the confinement potential due to band offset. $F(\mathbf{r})$ is the envelope wave function; and E is the carrier energy.

From eq. (2.2), by assuming the barrier potentials with *infinite height*, the carrier energy E and density of states per unit volume (D.O.S.) (the number of states

between the energy E and $E + dE$, of each quantum nanostructure) in the case of QD can be written as follows [33],

Assuming that the infinite confinement potential barrier in all direction, we get [33]

$$E_{QD} = E_{n_x} + E_{n_y} + E_{n_z} = \frac{\hbar^2}{2m^*}\left[\left(\frac{n_x\pi}{L_x}\right)^2 + \left(\frac{n_y\pi}{L_y}\right)^2 + \left(\frac{n_z\pi}{L_z}\right)^2\right] \tag{2.3}$$

$$D_{QD}(E) = 2N_D \sum_{n_x,n_y,n_z} \delta(E - E_{n_x} - E_{n_y} - E_{n_z}) \tag{2.4}$$

where δ is the delta function, and N_D is the volume density of QD.

The change of density of states for the low-dimensional nanostructures (figure 2.2) affects the fundamental properties of devices, which use these nanostructures as an active layer [36]. In the case of QD structures, there are several theoretical and experimental proofs that semiconductor lasers consisting of QD structures have the lowest threshold current density due to the delta-function-like density of states [37].

To utilize QDs as an active layer for semiconductor laser applications, the maximum optical gain (g^{sat}) for a QD laser should be considered [38];

$$g^{sat} \propto N_e/\Delta \tag{2.5}$$

where N_e is the number of states per unit surface area and Δ is the total spectrum broadening from all excited QDs. From eq. (2.5), it's possible to increase g^{sat} by increasing the QD density (to increase N_e) and/or reducing the QD size distribution.

2.1.2 Double potential well

The coupling of double potential well is briefly discussed in *"Quantum Wells, Wires & Dots" (Paul Harrison, 2005)*, using an example of GaAs/$Ga_{1-x}Al_xAs$ double potential wells. The simplest example of the former would be the symmetric double well of Figure 2.4. The potential function V(z) required for the numerical solution is simply the conduction band edge as given in figure 2.4.

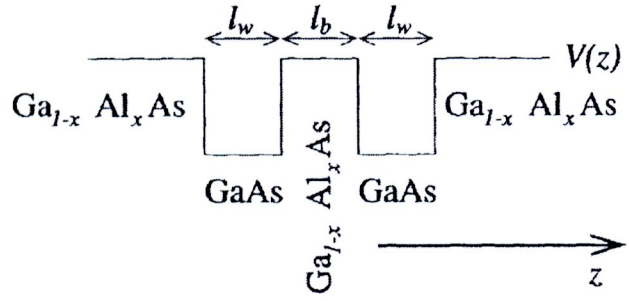

Figure 2.4 Band profile of symmetric GaAs/$Ga_{1-x}Al_xAs$ double potential well [39].

Figure 2.5 displays the results of calculations of the lowest two energy states as a function of the central barrier width for a double potential well with the Al barrier concentration x = 0.2 and a fixed well width l_w — 60 Å. When the wells are separated by a large distance, the interaction between the eigenstates localized within each well is very small and the wells behave as two independent single wells. However, as illustrated in Figure 2.5, as the central barrier l_b (corresponding to distance between two wells) is decreased, the energy levels interact, with one being forced to higher energies and the other to lower energies.

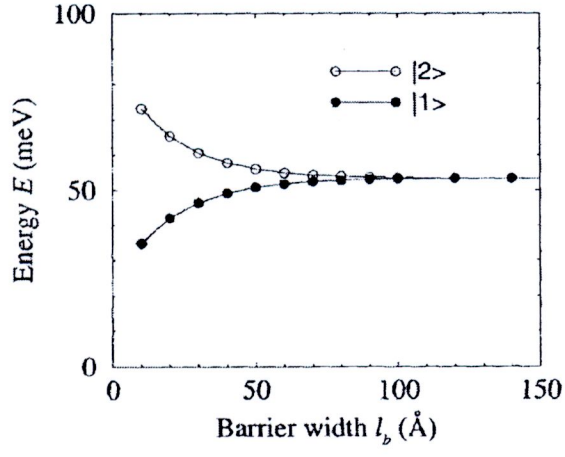

Figure 2.5 Confinement energies of the lowest two states of a symmetric double potential well as a function of the central barrier width [39].

In the case of the double potential well, a situation occurs with the electron spins aligning in an *anti-parallel* arrangement in order to satisfy the Pauli's exclusion principle. Figure 2.6 displays the wave functions of the double well with a central

barrier width of 40 Å. Clearly, they form a symmetric and anti-symmetric pair, with the former being of lower energy.

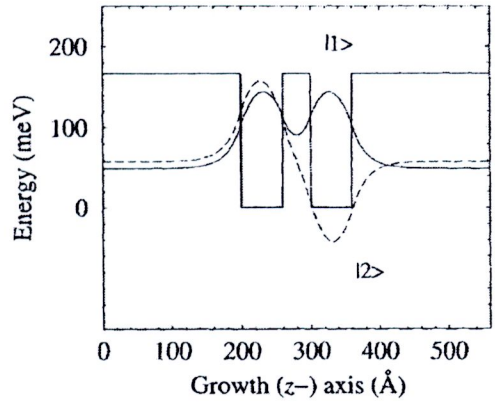

Figure 2.6 Wave functions of the lowest two energy levels of the symmetric double potential well with a central barrier width of 40 Å [39].

2.1.3 Ring-shaped nanostructures or quantum rings (QRs)

The ring-shaped nanostructures, so called quantum rings (QRs) are another type of quantum-confinement structure. Like QDs, QRs have their energy level quantized due to their confinement properties. This makes them potentially applicable in electronics, optics, and quantum information processing [8-10]. However, semiconductor quantum rings have attracted a great deal of attention because of their additional properties predicted and demonstrated [40,41]. For example, the ring-structures are a special class of quantum-confinement due to the Aharonov-Bohm effect, which is specific to the topology of a ring [42]. Also, interesting are magnetic properties of QRs, which are related to the possibility of inducing persistent current inside the structure when they are put into a magnetic field.

The persistent current of a quantum ring [43] can be written in general as

$$I(\Phi) = -\frac{\partial F}{\partial \Phi}, \tag{2.6}$$

where F is the free energy of the system and Φ the magnetic flux piercing the ring. At zero temperature, the free energy can be replaced with the ground state energy. The energy of a ring and consequently also the persistent current is a periodic function of

the flux. The effect of the magnetic field is to lower the energy states of high angular momentum with respect of those at low angular momentum [43]. When the flux is increased, the ground state energy will jump from one angular momentum to the next causing the periodic behavior.

2.1.4 Material Considerations

Mostly, the preliminary condition for the growth is that the nanostructure material has a smaller band gap compared with the matrix material(s) to provide a potential well in the energy band. Unlike the SK growth mode, the material for the nanostructure fabricated by droplet epitaxy does not necessarily have a larger or smaller lattice constant since the method can be applied to lattice-matched system such as AlGaAs/GaAs. Figure 2.7 shows the relationship between the band gap energy and the lattice constant of III-As material systems. There is a possibility to realize nanostructures which emit light at the wavelength of 1.3 μm or 1.55 μm (dashed lines).

For laser applications in optical communication systems, GaAs is the most important substrate material. The self-assembled growth of InGaAs on a GaAs substrate can provide the nanostructures which emit light at 1.3 μm or longer wavelength, depended on the ratio of In and Ga in the InGaAs structures. In this work, we shall concentrate only on the InGaAs/GaAs material system.

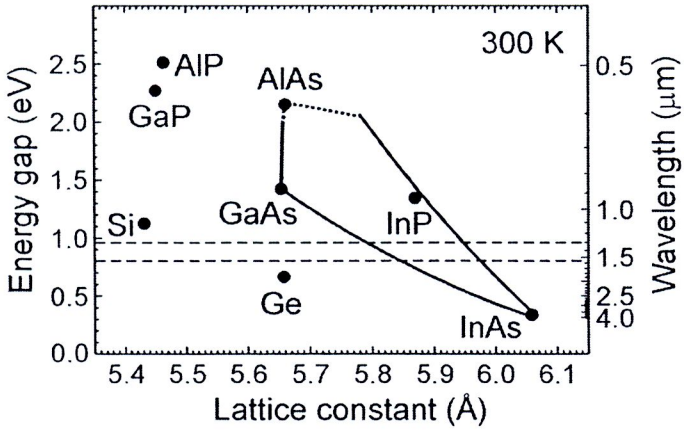

Figure 2.7 The relationship between lattice constant and energy gap at room temperature for the III-As material system. The solid line: direct band gap material, and the dotted line: indirect band gap material.

2.2 Self-assembled growth

The self-assembled growth can realize nanostructures such as QDs. The growth mode and growth conditions for self-assembled growth are briefly reviewed in order to provide some basic understanding of the growth method. Droplet epitaxy is also introduced as the fabrication technique used in this work.

2.2.1 Growth modes

To define the growth mode during the film deposition, $\Delta\gamma$ (the change of total energy of a surface before and after deposition) is considered:

$$\Delta\gamma = \gamma_F + \gamma_{S/F} - \gamma_S \tag{2.7}$$

where γ_S is substrate surface energy, γ_F is film surface energy, and $\gamma_{S/F}$ is interface energy between the grown film and the substrate including the additional energy arising from the strain between the film and the substrate.

If $\Delta\gamma > 0$, the deposited material would prefer to cover the substrate surface since the interaction between the substrate and deposited atoms is stronger than that between neighboring atoms. This is Frank Van der Merwe growth mode or layer-by-layer growth (figure 2.8(a)). If $\Delta\gamma < 0$, the interaction between the substrate and neighboring atoms exceeds the overlayer-substrate interaction, thus, the 3D Volmer Weber growth mode is observed (figure 2.8(c)).

THE NATIONAL RESEARCH COUNCIL OF THAILAND
RESEARCH LIBRARY

The National Research Council of Thailand
Research Library
Date 23 NOV 2012
Record No. E46262
Call No.

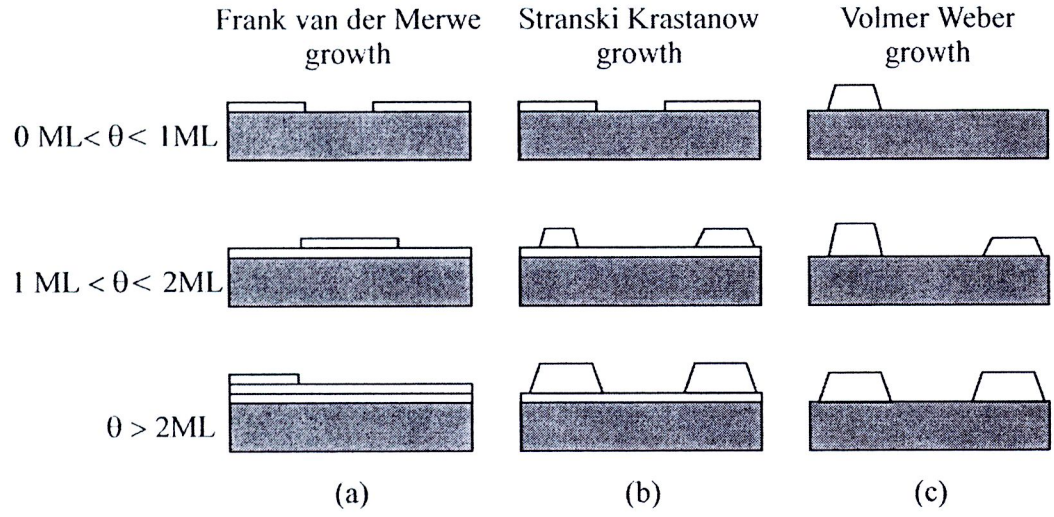

Figure 2.8 Schematic representation of the 3 important growth modes of a film for different coverage (θ) (a) Frank van der Merwe (FM), (b) Stranski Krastanow (SK), and (c) Volmer Weber (VM) [44].

In the intermediate case, the deposited film can grow a few monolayers in layer-by-layer growth mode at the early stage of deposition ($\Delta\gamma < 0$). However, due to the strain between the grown film and the substrate accumulating with the deposited film thickness, the islands are formed on top of the *intermediate* layer (the wetting layer (WL)) since $\Delta\gamma$ becomes less than zero and the growth mode changes from 2D-growth mode to 3D-growth mode. This is layer-plus-island growth in Stranski-Krastanov growth mode (Figure 2.8(b)) used in the growth of many conventional QDs [45,46].

Although this growth mode is not used to fabricate the nanostructures in this work, the detail of SK growth mode is briefly introduced to provide the basics of QD formation from strain-releasing in a lattice-mismatched system. The Stranski-Krastanow (SK) growth mode is widely used to fabricate defect-free self-assembled QD structures in the case of lattice-mismatched systems (lattice mismatch : $\varepsilon_0 > 7\%$). First, a few monolayers of strained material grow in the layer-by-layer growth mode. During the growth, the elastic strain energy builds up due to the lattice mismatch and increasing film thickness [47]. The island formation is energetically favorable if material beyond critical thickness is deposited, because the lattice can elastically relax compressive strain and thus reducing strain energy, as shown in figure 2.9. Beyond the critical thickness, the layer-by-layer growth is unfavorable so elastic strain relaxation

occurs. The local strain energy density of the SK-growth mode QD is schematically represented in figure 2.10.

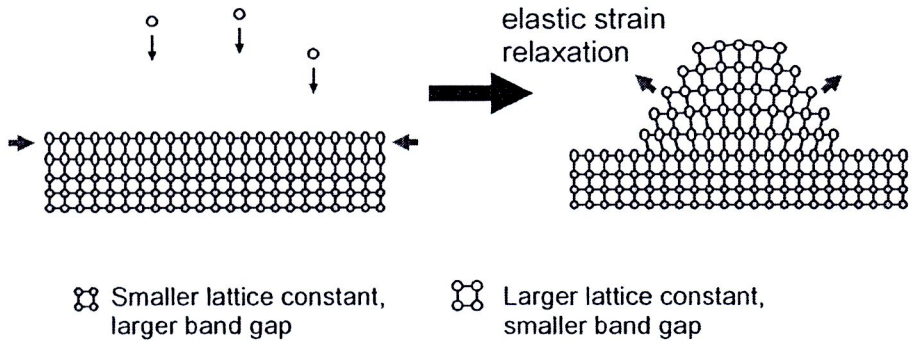

Figure 2.9 Illustration of island formation during epitaxial growth of a semiconductor material on the top of another semiconductor with a smaller lattice constant in Stranski-Krastanow mode.

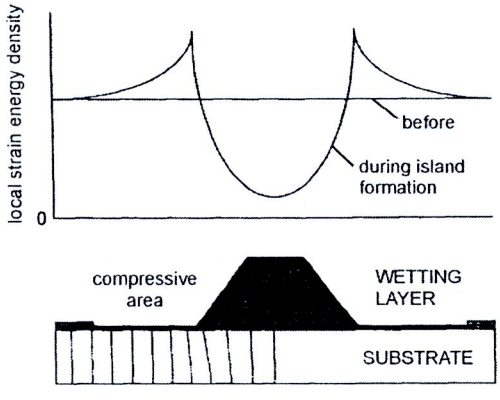

Figure 2.10 Schematic representation of the local strain energy density in and around the SK-growth mode QD. The energy barrier has a maximum at the edge of the QD [47].

Although the QDs grown by this technique form into high-density arrays. There are still some disadvantages of this technique. First, the SK growth mode QDs exhibit wide size distribution, varying the energy level in the energy band. Since, carriers in a small size QD would exhibit shorter de Broglie wavelength of which corresponding energy level is higher. The representations of the energy level exhibited in the QD with different size are shown in Figure 2.11. Also, the non-uniform strain

distribution from the lattice-mismatched formation would effect on the energy band structure of QD [48]. Both are undesirable for the laser applications.

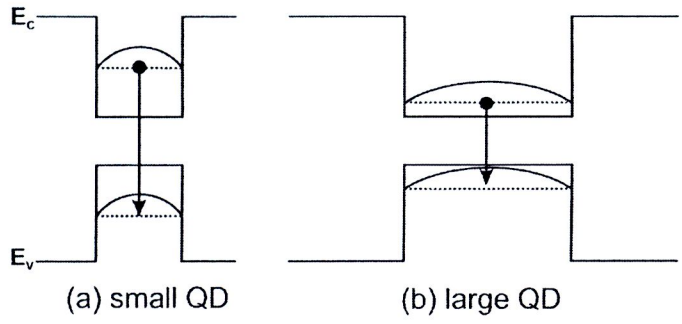

Figure 2.11 Simple interpretation of the energy level exhibited in the QD with different size. The representations in case of (a) small QD show the higher energy level than that of large QD, (b) due to the carrier confinement properties.

2.2.2 Droplet Epitaxy

Droplet epitaxy is an alternative approach of self-organized nanostructure fabrication which can be applied to both lattice-matched [22,49-52] and mismatched system. Unlike SK growth mode, the nanostructures fabricated by droplet epitaxy are originated directly from strain-free group III-element droplets formed on a crystalline III-V surface instead of strain-releasing in a lattice-mismatched system. Therefore, the strain-energy in the nanostructure and its effects on the energy-band structure are reduced due to the lattice-matched droplet formation. Thus, high-quality strain-less nanostructures can be fabricated by this technique, useful for the studies of semiconductor QR physics.

The droplet epitaxy process consists of 2 main steps. The illustration of the nanostructure fabrication by droplet epitaxy is shown in figure 2.12. First, group III metallic droplets are formed on a III-V compound substrate surface by depositing group III atoms on the substrate under the absence of group V. The formation mechanism of group III metallic droplets is explained by Volmer-Weber growth mode [44], in which the bonding energy between incoming group III adatoms is much higher than the bonding energy between the surface and the adatoms. Therefore, as soon as incidenting III-V surface, liquid In and Ga coalesce and form hemispherical droplets

(instead of layers). Second, the group III droplets are crystallized in group V molecular beam to form III-V compound nanostructures.

Since the III-V nanostructures are originated from respective droplets, the structural properties of the III-V compound nanostructures can be controlled by droplet forming parameters, such as substrate temperatures and amount of group III-element deposited. Since the droplet properties are still metallic, their morphology can be varied by changing such parameters. The crystallization conditions also affect the nanostructures.

However, there are limitations for the fabrication of InAs nanostructures on GaAs by droplet epitaxy such as very low density (~10^7-10^8 QRs/cm^2) and large size (~200-400 nm) [3,24] due to a too long 2-D migration length of In and high segregation effect of the newly supplied adatoms. To overcome these problems, the growth should be done at low temperature and use the optimum crystallization conditions [29]. Another solution is to limit the migration length of In atoms on a GaAs surface. Ga is also supplied together with the In deposition [53] and form InGa droplets. InGaAs nanostructures are formed after the crystallization.

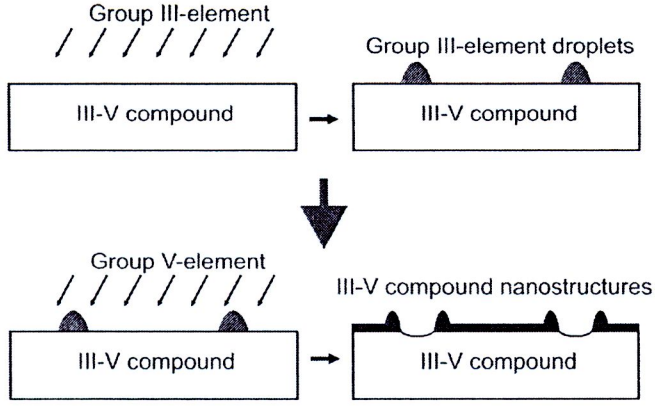

Figure 2.12 The illustration of the nanostructure fabricated by droplet epitaxy.

2.2.3 Migration-Enhanced Epitaxy (MEE)

Migration-enhanced epitaxy (MEE) of III-V compound semiconductors is useful for growing high quality epitaxial layers even at low substrate temperature (300°C-400°C). Unlike the conventional growth, the MEE growth proceeds in a layer-by-layer manner, based on alternately supplying group III atoms and group V to III-V

surface to obtain metal-stabilized surfaces, periodically. The shutter operation of MEE is shown in figure 2.13. In the growth of III-V compound semiconductors, the surface migration is effectively enhanced by supplying group III atoms to the growing surface in the absence of group V. Since, when the number of group III atoms supplied to the surface is much less than the number of surface sites, these atoms are quite mobile in the surface and do not cohere with each other to the surface site number. As a result, the lifetime of isolated group III atoms is greatly increased, resulting in these atoms migrating in a large distance along the surface, even at low temperature [44,54].

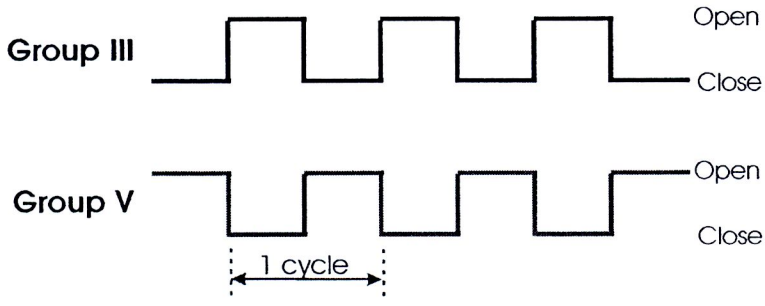

Figure 2.13 Shutter operation characteristic of migration-enhanced epitaxy (MEE).